Ranging Property of the Dual-Band Band Limited Signal (DBBLS)

Pavel KOVÁŘ, Petr KAČMAŘÍK
The Czech Technical University in Prague, Czech Republic
Faculty of Electrical Engineering, Technická 2, 166 27 Prague 6
kovar@fel.cvut.cz

***Abstract*—The Dual-Band Band Limited Signal (DBBLS) is a signal with its power spectral density consisting of two separate lobes. Signals that can be considered as DBBLS are for example signals with BOC, AltBOC modulation, signals modulated on two close carriers and many other signals, which are used in modern satellite navigation systems. This signal advantage is its excellent ranging property. The parted power spectral density enables processing the DBBLS as a single wideband signal in single-channel receiver or as two narrow band signals in two-channel receiver. The signal processing of the ranging signals is based on the calculation of the cross-correlation function, which can be calculated from the signal measured by the two-channel receiver by the derived method more efficiently than from the whole signal. The two-channel processing has nearly optimal performance, but the hardware and computation complexity is much lower. The developed method can by applied, for instance, for the processing of the Galileo E5 signal or pair of the Compass L1 signals.**

***Index Terms*—BOC, GNSS, Navigation, Ranging, Signal processing, Signal sampling.**

I. Introduction

Modern satellite and terrestrial navigation systems mostly utilize a ranging navigation method based on the wideband radio signals optimized for time of arrival measurement. The suitable signals are Direct Sequence Spread Spectrum signals that are used in global navigation satellite systems (GNSS). The navigation systems traditionally implement the BPSK (binary phase-shift keying) or QPSK (quadrature phase-shift keying) modulation by the ranging code and the navigation message [6]. The new or modernized systems like Galileo or GPS III apply some modification of the BOC (binary offset carrier) modulation [1]. The GPS introduces military signals (M-signals) [2] that have power spectral density consisting of two separate components symmetrically placed around the carrier frequency. Similar type of the navigation signal was tested in China's Compass system on L1 frequency [3].

The time of arrival of the navigation signal and carrier phase are standardly estimated by the delay lock loop (DLL) and phase lock loop (PLL) [7]. The processing methods of the BPSK, QPSK and BOC navigation signals are published in many books and papers [4, 5, 6, 7], while the information of the processing of the GPS military signals and Compass signals is not publicly available.

The key problem in the design of the GNSS receiver for wideband signals is a design of the computationally efficient signal processing. For instance in [11] is patented the computationally efficient realization of the discriminator function of the signal modulated on single and multiple carriers. The patent [12] describes receiver architecture for the signal modulated on two carrier waveforms.

This paper studies signal processing of the ranging signals with spectrum consisting of two separate components, see Fig. 1., with the aim of saving the computation complexity and improving the signal processing robustness. The studied signal is called in this paper as the Dual-Band Band Limited Signal (DBBLS). The simplification is reached by the utilization of the two-channel receiver and processing.

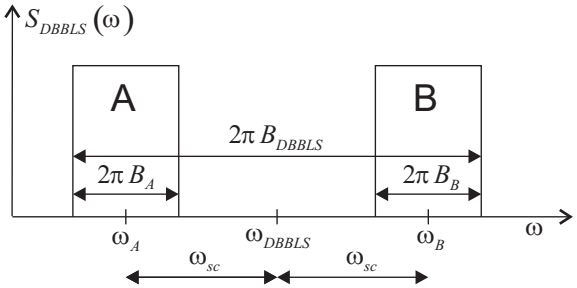

Figure 1. One-sided spectrum of the dual-band band limited signal (DBBLS)

II. Double-Band Band Limited Signal

Fig. 1. shows the power spectral density of the Dual-Band Band Limited Signal (DBBLS). The power spectral density consists of two band limited spectral components **A** ($S_A(\omega)$) and **B** ($S_B(\omega)$) which are not overlapped. Outside of these components, the power spectral density is equal to zero. The term ω_{DBBLS} is an angular carrier frequency of the DBBLS signal.

We additionally assume that the central frequencies (sub carrier frequencies) ω_A of component **A** and ω_B of **B** have the same distances from the carrier frequency ω_{DBBLS} ($\omega_{DBBLS} - \omega_A = \omega_B - \omega_{DBBLS} = \omega_{sc}$). In other words, the DBBLS consists of two ranging signals **A** and **B** modulated on the carrier frequencies $\omega_{DBBLS} - \omega_{sc}$ and $\omega_{DBBLS} + \omega_{sc}$.

The time representation of **A** component is given $s_A(t) = \mathrm{F}^{-1}\left[S_A(\omega)\right]$ and **B** component is $s_B(t) = \mathrm{F}^{-1}\left[S_B(\omega)\right]$, where $\mathrm{F}^{-1}[.]$ is an operator of the inverse Fourier transform. The bandwidth of the DBBLS signals is B_{DBBLS} while the bandwidths of **A** and **B** components are B_A and B_B ($B_{DBBLS} < B_A + B_B$).

This work was supported by the grant SGS12/152/OHK3/2T/13 "Efficient GNSS Signal Processing" of the Czech Technical University in Prague.

Digital Object Identifier 10.4316/AECE.2012.03014

The reason why we introduce DBBLS signal is to cope with the signal processing for two different receiver setups:

1. **Single-channel receiver (method)** that processes whole signal of bandwidth B_{DBBLS},
2. **Two-channel receiver (method),** which processes the same signal, but divided into two signals of bandwidth B_A and B_B.

The two-channel method has several advantages over the single-channel one. The main advantage is its lower processing bandwidth $B_A + B_B < B_{DBBLS}$ and thus much lower sampling frequency for the analog to digital conversion because the signal can be digitized in the channels **A** and **B** separately. The comparison of the two-channel and single-channel methods from the perspective of the receiver front-end design is analyzed in Chapter IV.

In addition, the two-channel method enables to process both signal components cooperatively. This method is called as **two-channel cooperative method (processing)** and is described in the next paragraphs together with the second method that processes each signal components separately. The second method is called as **piecewise method (processing)**. The resulting pseudo-range acquired by the piecewise method can be measured on the one of the components **A** or **B** or these independent measurements can be combined with the single pseudo-range.

The two-channel receiver is very flexible, because it can adaptively switch between the more precise but less robust two-channel cooperative method and the less precise but more robust piecewise method.

III. Correlation Function of the DBBLS

In this paragraph, we derive the formula of DBBLS correlation function, as this knowledge is crucial for the design of the delay discriminator for the DLL and the phase discriminator for the PLL.

The complex envelope of the DBBLS signal (with the carrier frequency ω_{DBBLS}) is given by

$$\tilde{s}_{DBBLS}(t) = \tilde{s}_A(t)e^{-j\omega_{sc}t} + \tilde{s}_B(t)e^{j\omega_{sc}t}. \quad (1)$$

where $\tilde{s}_A(t)$ is the complex envelope of the component **A** for the central frequency ω_A and $\tilde{s}_B(t)$ is the complex envelope of the component **B** for the central frequency ω_B.

We additionally assume that the auto-correlation functions of $\tilde{s}_A(t)$ and $\tilde{s}_B(t)$ are identical $R_A(\tau) = R_B(\tau)$.

The cross-correlation function of the DBBLS signal and DBBLS signal affected by the unknown phase shift φ is given by

$$R_{DBBLS}(\tau) = \int_{T_I} \tilde{s}_{DBBLS}(t)e^{j\varphi}\tilde{s}^*_{DBBLS}(t+\tau)dt = e^{j\varphi}\int_{T_I}\left[\begin{array}{l}\left(\tilde{s}_A(t)e^{-j\omega_{sc}t} + \tilde{s}_B(t)e^{j\omega_{sc}t}\right)\cdot \\ \left(\tilde{s}^*_A(t+\tau)e^{j\omega_{sc}(t+\tau)} + \tilde{s}^*_B(t+\tau)e^{-j\omega_{sc}(t+\tau)}\right)\end{array}\right]dt \quad (2)$$

As $\tilde{s}_A(t)$ and $\tilde{s}_B(t)$ signals are uncorrelated (their spectra are not overlapped), we can simplify equation (2)

$$R_{DBBLS}(\tau) = e^{j\varphi}\left[\begin{array}{l}e^{j\omega_{sc}\tau}\int_{T_I}\tilde{s}_A(t)\tilde{s}^*_A(t+\tau)dt + \\ +e^{-j\omega_{sc}\tau}\int_{T_I}\tilde{s}_B(t)\tilde{s}^*_B(t+\tau)dt\end{array}\right] = e^{j\varphi}\left[e^{j\omega_{sc}\tau}R_A(\tau) + e^{-j\omega_{sc}\tau}R_B(\tau)\right] \quad (3)$$

We apply assumption of $R_A(\tau) = R_B(\tau)$ and we obtain

$$R_{DBBLS}(\tau) = 2e^{j\varphi}R_A(\tau)\cos(\omega_{sc}\tau). \quad (4)$$

The term $2R_A(\tau)\cos(\omega_{sc}\tau)$ is an auto-correlation function of the DBBLS signal. The alternation rate of the auto-correlation function $R_A(\tau)$ is due to $B_A < 2\omega_{sc}$ lower than the alternation rate of $\cos(\omega_{sc}\tau)$. The auto-correlation function of the **A** signal component is an envelope of the auto-correlation function of the DBBLS signal, see Fig 2.

The signal parameters used for drawing of the correlation function in Fig. 2, the delay discriminator characteristics in Chapter V (Fig. 7, Fig. 8) and the performance simulation in Chapter VII corresponds with the Compass signal on frequency L1 [3]. The signal is modulated onto two sub-carriers, $f_{sc} = 14,32$ MHz, by QPSK(2) modulation, i.e. QPSK modulation of the chip rate 2046 kchip/s. The **A** and **B** components are band limited by the digital filter of bandwidth 4 MHz.

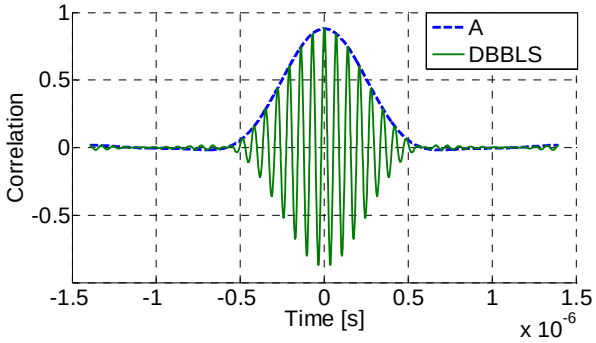

Figure 2. Auto-correlation function of the DBBLS signal

IV. Front-End for DBBLS

The DBBLS signal can be received by the various front-ends. In this paragraph, we propose several variants of the front-ends and analyze their complexity, sampling frequency f_s (angular sampling frequency $\omega_s = 2\pi f_s$) of the output signal and the impact on the next processing in the receiver.

A. Single channel front-end

The single-channel front-end processes the DBBLS signal in the single radio frequency chain. The frequency characteristic of this front-end passes the whole signal. The single-channel front-end can use various receiver architectures:

- **Superheterodyne receiver**, which converts received signal onto the intermediated frequency (IF) for effortless filtration, amplification and conversion to the digital domain,
- **Direct-conversion receiver,** which directly transforms the received signal to the complex (I & Q) baseband signal (complex envelope),

- **Pure software receiver,** in which the amplified and filtered signal received by the antenna is directly digitized by the ADC and then processed digitally.

There are two methods for the analog to digital conversion of the receiver output signals, the IF sampling and the baseband sampling. The IF sampling method processes the output signal, see Fig. 3a, directly on the carrier frequency (pure software receiver front-end) or on the intermediated frequency (superheterodyne receiver). The sampling frequency must be at least twice of *N* dB receiver bandwidth B_{IF_N}, see Fig. 3b.

The baseband sampling method requires conversion of the processed signal to the complex baseband signals (complex envelope), see Fig. 3c. The appropriate signal is at the output of the direct conversion receiver. In case of the superheterodyne receiver, the output intermediated signal has to be transformed to the appropriate form by the quadrature demodulator. The baseband signal is then processed by the pair of ADCs. The sampling frequency must be at least twice higher than *N* dB bandwidth of the receiver bandwidth B_{BB_N}, see Fig. 3d.

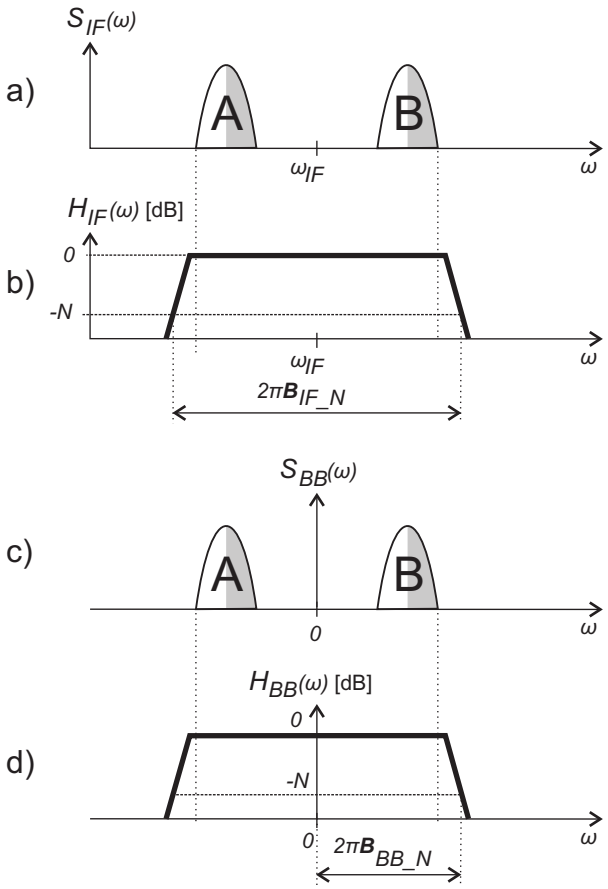

Figure 3. a) one-sided spectrum of the DBBLS on intermediate frequency, b) one-sided frequency response of the intermediate frequency amplifier with marked *N* dB bandwidth c) two-sided spectrum of the complex baseband DBBLS signal d) two-sided frequency response of the direct conversion receiver with marked *N* dB bandwidth

As the bandwidth of the baseband signal is half of the bandwidth of the carrier frequency signal, the baseband sampling requires approximately half sampling rate than the IF sampling of the same signal. On the other hand the IF sampling processes the real signal (one ADC), but the baseband sampling processes the complex signal and thus the two-channel ADC is needed.

The described front-ends do not affect (distort) the signal if there are used filters with a constant group delay and a constant amplitude response for the passband frequencies.

If the subcarrier frequency ω_{sc} is high compared to the **A** or **B** component bandwidth, the receiver can utilize smaller sampling frequency in comparison to B_{IF_N} case. Let us assume frequency response of the receiver and DBBLS signal spectrum according to Fig 4a and Fig 4b, respectively. For such signal with ω_{IF} we can find a sampling frequency ω_s for which the spectral components **A** and **B** of sampled signal are not overlapped. The mutual positions of these components on the frequency axis are now changed by the sampling, see Fig. 4c. That is why the sampled signal cannot be processed as a whole DBBLS signal by single-channel method, but by the two-channel cooperative method or piece-wise method described in Chapter IVb. We name this sampling method the **DBBLS economic sampling**.

This method is applicable for signals which meet the inequality $B_{DBBLS} > 3.B_A$. The **B** component for signals with large B_{DBBLS}/B_A ratio can be located in $N+2$ or higher zone.

This sampling method is based on a multi-frequency GNSS signal sampling in the pure software GNSS receivers developed by [8].

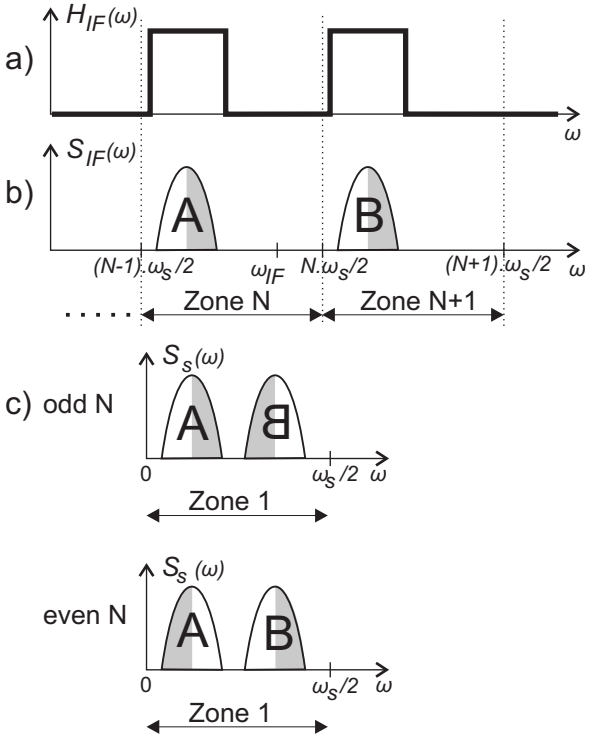

Figure 4. Dual band economic sampling a) idealized frequency response of the intermediate frequency amplifier b) DBBLS one-sided spectrum c) one-sided spectrum of the sampled signal

B. Two-channel front-end

The cross-correlation function of the received signal and the locally generated replica can be calculated by the sum of two terms, see (3). The first term is an appropriately rotated

cross-correlation function of $s_A(t)$ and second one is an appropriately rotated cross-correlation function of $s_B(t)$. For realization of this operation, we need to know the frequency and phase relationships in both channels otherwise the method cannot be used and the signal must be processed by the less precise piece-wise method. In other words, for application of the two-channel cooperative method we need knowledge of the precise phase and frequency of the local oscillators in both **A** and **B** channels and the phase shifts in both channels. The control of the frequency of the local oscillator is not a problem if the frequency synthesizers are controlled by the same frequency standard. On the other hand, it is difficult to keep the reliability of the phase conditions. Despite the fact that the phase delays of both channels can be calibrated in the already produced receiver, the temperature and other environment variations can cause addition uncalibrated phase error. In addition, the phase of the signal generated by the conventional synthesizer depends on the unknown initial state of the digital divider.

The cross-correlation function of the DBBLS for unknown phase error φ_{eA} of the component **A** and φ_{eB} of **B** is given by

$$\begin{aligned} &R'_{DBBLS}(\tau) = \\ &e^{j\varphi}\int_{T_I}\left[\begin{array}{l}\left(\tilde{s}_A(t)e^{-j(\omega_{sc}t+\varphi_{eA})}+\tilde{s}_B(t)e^{j(\omega_{sc}t+\varphi_{eB})}\right)\cdot\\ \left(\tilde{s}_A^*(t+\tau)e^{j\omega_{sc}(t+\tau)}+\tilde{s}_B^*(t+\tau)e^{-j\omega_{sc}(t+\tau)}\right)\end{array}\right]dt = \\ &e^{j\varphi}R_A(\tau)\left[e^{-j(\omega_{sc}\tau+\varphi_{eA})}+e^{j(\omega_{sc}\tau+\varphi_{eB})}\right] = \\ &e^{j\left(\varphi+\frac{\varphi_{eA}-\varphi_{eB}}{2}\right)}R_A(\tau)\left[e^{j\left(\omega_{sc}\tau+\frac{\varphi_{eB}-\varphi_{eA}}{2}\right)}+e^{-j\left(\omega_{sc}\tau+\frac{\varphi_{eB}-\varphi_{eA}}{2}\right)}\right] = \\ &2e^{j\left(\varphi+\frac{\varphi_{eA}-\varphi_{eB}}{2}\right)}R_A(\tau)\cos\left(\omega_{sc}\tau+\frac{\varphi_{eB}-\varphi_{eA}}{2}\right)\end{aligned} \quad (5)$$

The phase errors φ_{eA} and φ_{eB} cause not only the phase shift of the correlation function of angle $\frac{\varphi_{eA}-\varphi_{eB}}{2}$, but also the time shift of the cross-correlation function peak by $-\frac{\varphi_{eB}-\varphi_{eA}}{2\omega_{sc}}$. This shift causes systematic bias of the pseudo-range measurement for all DBBLS signals. These biased pseudoranges cannot be directly combined with non-bias piecewise pseudoranges. The solution of this problem caused with unknown phase errors in the two-channel front-end which is based on its estimation by the Kalman filter is outlined in Chapter VI.

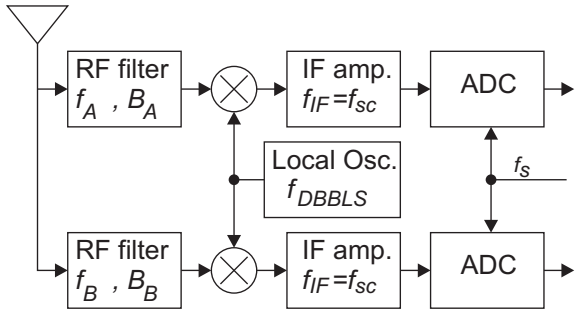

Figure 5. Two-channel front-end with common local oscillator

The two-channels front-end can be realized by two independent front-ends based on the superheterodyne or the direct conversion receiver architecture with stand-alone local oscillators. The local oscillator synthesizers must be controlled with the same frequency standard in this case. The second front-end solution with the common local oscillator drawn in Fig. 5. guarantees deterministic phase of the local oscillator signals, but the drawback is that the receiver is specially designed for given signal only, thus the flexibility (applicability on other signals) is very poor.

The last problem of the two-channel front-end discussed here is an amplitude unbalance of the channels. The influence of this receiver imperfection to the delay and phase discriminator characteristics is analyzed in Chapter V.

C. Partial Conclusion

The single-channel front-end has no problem with the unknown phase shift of the **A** and **B** components, but it requires much higher sampling frequency than the two-channel front-end. In addition, the digital signal processor has to process higher number of samples and hence it is more complicated than the signal processor for processing of the two-channel front-end samples.

The realization of the wide bandwidth single-channel front-end is rather complicated. It requires higher order filter for the same suppression of the out of band signals than the two-channel one. In addition, the two-channel front-end is featured with higher robustness. The high-level interference in one-channel blocks reception in this channel, but the signal in the other channel can by received and processed without distortion. The same interference can totally block the reception of the signal in the single-channel front-end.

V. CORRELATOR, PHASE AND DELAY DISCRIMINATORS

The GNSS signals are ordinarily processed by the DLL and PLL loops that realize reiterative maximum likelihood (ML) estimation of the signal delay τ and phase φ [6, 7]. The key parts of the DLL and PLL are delay and phase discriminators, which indicate the deviation from the cross-correlation function maximum and the phase error of the received signal carrier.

A. Standard delay and phase discriminators

The overview of the standard delay discriminators is in Table I. and the phase discriminators in Table II. [6]. The mentioned discriminators compare the *E* (early), *P* (prompt) and *L* (late) correlator outputs, which are given by

$$\begin{aligned} E &= \int_{T_I}\tilde{s}_r(t)\tilde{r}^*\left(t+\tau+\frac{\Delta}{2}\right)dt \\ P &= \int_{T_I}\tilde{s}_r(t)\tilde{r}^*(t+\tau)dt \\ L &= \int_{T_I}\tilde{s}_r(t)\tilde{r}^*\left(t+\tau-\frac{\Delta}{2}\right)dt \end{aligned} \quad (6)$$

where $\tilde{s}_r(t)$ is a complex envelope of the received signal, $\tilde{r}(t)$ is a signal replica (known part of the transmitted signal), Δ is a correlator spacing and τ is a replica delay. The E, P and L are values of the cross-correlation

function for the replica delays $\tau-\frac{\Delta}{2}$, τ and $\tau+\frac{\Delta}{2}$.

We assume that the replica ambiguity caused by the unknown navigation message bits has been resolved. This ambiguity solution is out of the scope of this paper. The solution of these ambiguities is well known for the BPSK modulated signals [6], the QPSK signal can be processed as an orthogonal pair of the BPSK signals. The solution of the ambiguity problem for more complex modulations like the Galileo AltBOC is in [10], [4].

The correlator spacing Δ is typically set to one chip of the ranging code for the BPSK or QPSK modulated signal. The typical value for the BOC modulated signal is half of the subchip $T_{sc}/2=\pi/\omega_{sc}$. Some special correlators, for instance narrow correlator [5], are featured with much lower correlator spacing.

TABLE I. STANDARD DELAY DISCRIMINATORS

Mark*	Discriminator algorithm	Name	Note
DD1	$\mathrm{Re}[E]-\mathrm{Re}[L]$	Coherent	Coherent
DD2	$\lvert E\rvert^2-\lvert L\rvert^2$	Early Power Minus Late Power	Non-coherent
DD3	$\frac{\lvert E\rvert^2-\lvert L\rvert^2}{\lvert E\rvert^2+\lvert L\rvert^2}$	Normalized Early Power Minus Late Power	Non-coherent
DD4	$\lvert E\rvert-\lvert L\rvert$	Early Envelope Minus Late Envelope	Non-coherent
DD5	$\mathrm{Re}[E-L]\mathrm{Re}[P]+\mathrm{Im}[E-L]\mathrm{Im}[P]$	Dot Product Power	Non-coherent

*Reference mark for text simplification

TABLE II. STANDARD PHASE DISCRIMINATORS

Mark	Discriminator algorithm	Note
PD1	$\mathrm{Im}[P]$	Phase discriminator
PD2	$\mathrm{ATAN2}(\mathrm{Im}[P],\mathrm{Re}[P])$	Phase discriminator
PD3	$\mathrm{sign}(\mathrm{Re}[P]).\mathrm{Im}[P]$	Costas loop discriminator
PD4	$\mathrm{Re}[P]\mathrm{Im}[P]$	Costas loop discriminator
PD5	$\frac{\mathrm{Re}[P]}{\mathrm{Im}[P]}$	Costas loop discriminator

B. E, P and L correlator implementation

The digital hardware implementation of the *E*, *P* and L signal replica generation is as follows:

1. Single *E* replica generator, the *P* and *L* replicas are obtained from the delay registers, see Fig. 6a. The *E*-*P* spacing $\frac{\Delta}{2}$ must be equal to the integer multiple of the sampling period ($N.T_s=\frac{N}{f_s}\overset{!}{=}\frac{\Delta}{2}$).
2. Three *E*, *P* and *L* replica generators, see Fig 6b
3. Hardware implementation of P correlator only. The *E* and *L* correlator outputs can be calculated by the approximate formulas derived further.

The first replica generation method is not favorable for the two-channel cooperative method because of the necessity of high sampling frequency to reach the required *E*-*L* correlator spacing Δ. The sampling theorem requires much lower sampling frequency for the **A** and **B** processing.

The second method has no restriction for the sampling frequency caused by the correlator spacing, but it requires three replica generators, one for the *E* replica, second one for the *P* replica and the last one for the *L* replica.

The third hardware saving method calculates the *E* and *L* correlator outputs by the special formulas that are derived here. The cross-correlation function of the DBBLS signal is given by formula (3), i.e. by the sum of two terms. The first term P_A is calculated from the **A** signal and the second term P_B is calculated from the **B** signal. The *P* correlator output is then given by

$$P_{DBBLS}=P_A+P_B \tag{7}$$

In vicinity of the correlation function maximum, the correlation function $R_A(\tau)$ of the component **A** and **B** is flat, see Fig. 2, so we can replace it by value $R(0)$ and we obtain the approximate formula

$$R_{DBBLS}(\tau)\doteq e^{j\varphi}\left[e^{j\omega_{sc}\tau}R_A(0)+e^{-j\omega_{sc}\tau}R_A(0)\right] \tag{8}$$

The *E* and *L* correlator outputs providing this condition are given by

$$\begin{aligned} E&=e^{-j\omega_{sc}\frac{\Delta}{2}}P_A+e^{j\omega_{sc}\frac{\Delta}{2}}P_B \\ L&=e^{j\omega_{sc}\frac{\Delta}{2}}P_A+e^{-j\omega_{sc}\frac{\Delta}{2}}P_B \end{aligned} \tag{9}$$

The formulas require separate measurement of P_A and P_B components.

In the next part of the paper, we call the measured *E* and *L* correlator outputs as **true *E* and *L* outputs** or values, while the correlator outputs calculated by formulas (9) are designated as **calculated**.

C. Delay discriminators for DBBLS

The two-channel cooperative method of the DBBLS signals enables to design new types of the coherent and non-coherent delay discriminators, see Tab. III, which utilize the *P* correlator output only.

TABLE III. DBBLS DELAY DISCRIMINATORS

Mark	Discriminator algorithm	Note
DD6	$\mathrm{Im}\left[P_A+P_B^*\right]$	Coherent
DD7	$\arg\left(P_A+P_B^*\right)$	Coherent
DD8	$\mathrm{Im}\left[\frac{P_A}{P_B}\right]$	Non-coherent
DD9	$\mathrm{ATAN}\left[\frac{P_A}{P_B}\right]$	Non-coherent

The proposed non-coherent delay discriminators for the DBBLS de facto compare the phase of P_A and P_B components and indicate the position of the maximum that arises when both components have the same phase (they are added in phase). The function of the coherent DBBLS delay discriminators is similar to non-coherent one, but they operate under assumption of phase synchronization.

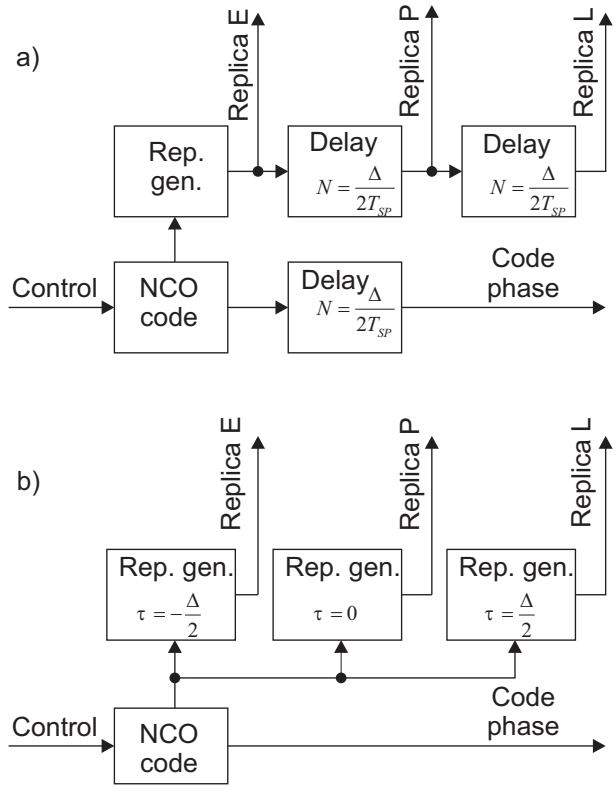

Figure 6. Signal replica generation

D. Discriminator characteristics and property

The discriminator characteristics for the DBBLS signal with QPSK(2) modulation, bandwidth B_A 4 MHz and sub-carrier frequency 14.32 MHz are drawn in Fig. 7 and 8. The differences between the discriminator characteristics DD1 – DD5 that utilize true *E* and *L* values and calculated *E* and *L* values are very small, so in the figures the true output version is shown only.

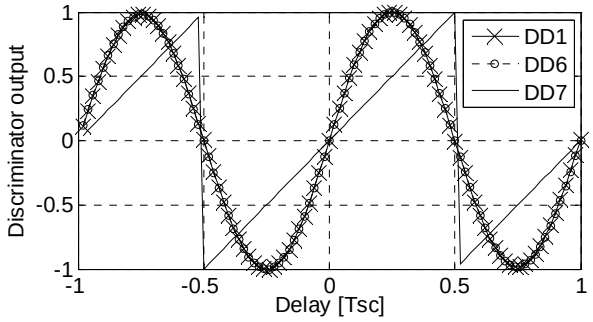

Figure 7. Coherent delay discriminator characteristics

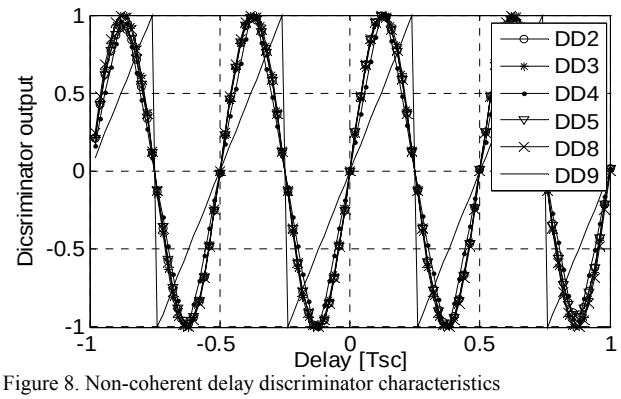

Figure 8. Non-coherent delay discriminator characteristics

The discriminator characteristics has several stable nodes as the correlation function (Fig. 2) has several adjacent peaks. Before closing the tracking loop the phase of the signal replica must be properly initiated to the vicinity of the correct peak. Moreover, the verification of the tracking of the correct correlation peak must be checked during a signal tracking. This initiation and verification problem is out of the scope of this paper. The solution is outlined in [4, 10].

The zone of uniqueness of the coherent discriminators is twice wider than the zone of uniqueness of the non-coherent ones as the non-coherent discriminators are not able to distinguish between positive and negative correlation peaks while coherent discriminators are capable of that.

The next investigated property is a behavior of the delay discriminators when the carrier phase is not perfectly synchronized and the amplitude responses of the channel **A** and **B** are not equal (channels are unbalanced). We investigated occurrence of the systematic tracking errors caused by these phenomena. The results are summarised in Tab. IV. The systematic tracking errors were observed for discriminators according Tab. I and III where the combination of the amplitude unbalance and carrier synchronization error were presented.

TABLE IV. SYSTEMATIC ERROR CAUSED BY A COMBINATION OF THE CARRIER SYNCHRONIZATION ERROR AND THE AMPLITUDE UMBALANCE OF THE CHANNELS A AND B

Mark	Systematic error
DD1	Yes
DD2	No
DD3	No
DD4	No
DD5	Yes
DD6	Yes
DD7	Yes
DD8	No
DD9	No

E. BOC modulation

The new and modernized GNSS systems widely use BOC type modulation instead of the traditional BPSK or QPSK ones because of its better ranging quality. The principal difference between the BOC modulated ranging signals and the DBBLS signals is in the utilization of different sub-carrier wave. The BOC applies some form of the rectangular wave while the DBBLS utilizes the harmonic one. The spectrum of the BOC modulate signals are theoretically unlimited, but in practical systems the signals are band-limited at the transmitter and in the receiver. The band-limitation distorts rectangular waveform and rounds its raising and falling edges.

The paper [14] analyzes losses of the precision of the range measurement of the band-limited BOC signals when the simplified replica with the harmonic sub-carrier wave is used. The observed implementation losses are very small.

The paper [13] studies implementation of the two-channel cooperative processing of the Galileo E5 signal with AltBOC modulation and compares it with the optimal processing method. The implementation losses of the two-channel methods obtained by the computer simulation were small especially for good signal to noise ratio corresponding with the outdoor reception while the signal processor complexity is about six times lower than the optimal one.

It is evident that the band limited BOC modulated signal

can be processed as the DBBLS by proposed methods including two channel cooperative methods that enable to combine various receiver front-end architectures, delays discriminators and methods for calculation of the correlation function.

One of the possible combinations is described in [11], which patents system for processing of the signal modulated on one or several frequencies. The system uses single channel front-end, but the cross correlation function is calculated by the two-channel method. The system uses true *E* and *L* correlator outputs and implements DD3 delay discriminator.

The other special case is published in [12]. The system is designed for processing the Galileo E5 signal and utilizes two-channel front-end with common local oscillator according to Fig. 5. The differences of the phase transfer of the front-end channels are calibrated. The signal processing is based on the two-channel cooperative method; the true *E, P* and *L* correlator values are used.

VI. Solution of the Phase Uncertainty of the Two-Channel Front-End

The DBBLS signal processing by the two-channel front-end is affected by the unknown phase unbalance between channels, which causes systematic tracking error (bias) r_e when the two-channel cooperative method is implemented. The error is $r_e = -\frac{\varphi_{eB} - \varphi_{eA}}{2\omega_{sc}}$, see Chapter IVB and formula (5). The less precise piecewise measurement is unbiased. The solution of this problem is to estimate and compensate this bias from the piecewise measurement.

The phase delays of the receiver channels depend on many environmental factors, especially on the temperature. As the ambient temperature changes, the error r_e is not constant, but it slightly varies in time.

The appropriate estimation method for r_e is the Kalman filter. The application of the Kalman filter requires to develope a system dynamic model of the estimated parameter (r_e in our case) and a model of the measurement.

The dynamic model of r_e can be based on the modeling of the rate of changing $v_e(n) = r_e(n) - r_e(n-1)$ by the first order Markov process.

$$\begin{bmatrix} r_e(n) \\ v_e(n) \end{bmatrix} = \begin{bmatrix} 1 & \alpha \\ 0 & 1 \end{bmatrix} \begin{bmatrix} r_e(n-1) \\ v_e(n-1) \end{bmatrix} + \begin{bmatrix} 0 \\ q_v(n) \end{bmatrix} \tag{10}$$

The estimation of r_e can be realized from a single satellite measurement or from the measurement to all satellites. The implementation of the estimation method based on the single satellite measurement is less complex. We can simplify model of the measurement.

$$\begin{aligned} r_m &= r_{DBBLS} - r_{piecewise} \\ r_m &= r_e + w_m \end{aligned} \tag{11}$$

where w_m is the error of the measurement, which can be approximated by the error of the piecewise measurement as the BDDLS measurement error is much lower.

The estimation of r_e from all satellites is appropriate to implement directly to the Kalman filter for the PVT (position, velocity, time) estimation. The PVT filter is extended by another estimated parameter r_e.

The implementation of the proposed methods for estimation of r_e requires equipping the two-channel front-end navigation receiver with the signal processor capable to process signals by the two-channel cooperative method and the piecewise method simultaneously.

VII. Simulation Results

This part of the paper incorporates simulation results of the processing of the DBBLS signal. The tracking errors of the single-channel, two-channel cooperative and two-channel piecewise methods, for delay discriminators from Table I. and Table III. have been investigated and compared. For the delay discriminators from Table I. we tested the true and calculated *E* and *L* correlators outputs.

To obtain commensurable results, the gain of the delay discriminators was calibrated for noiseless signal.

The comparison of the single-channel, two-channel cooperative and piecewise methods is in Fig. 9. The large frequency distance of the **A** and **B** sub-carriers and the relatively slow ranging code rate explains the considerable reduction of the pseudorange error of the single-channel and two-channel cooperative methods in comparison to the piecewise ones.

The similar comparison for the Galileo E5 signal is in [5], where the improvement is not so significant due to the higher chip rate of the pseudorandom codes.

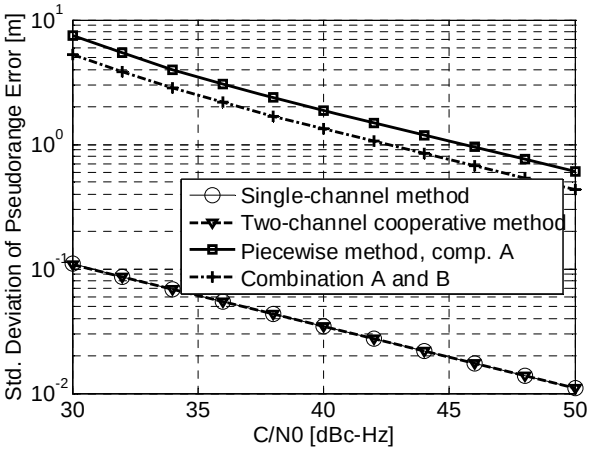

Figure 9. Comparison of the single-channel, two-channel cooperative and piecewise methods (discriminator DD1) and pseudorange estimated from the combination of the piecewise measurements in channels **A** and **B**, B_n = 3 Hz, T_I = 4 ms.

In Fig 10, there is an example of the comparison of the performance of the two-channel method utilizing true *E* and *L* correlator outputs and two-channel method with calculated *E* and *L* correlator outputs. The figure is drawn for discriminator DD1. The performance of both variants is practically identical. The identical performance is also obtained when comparing the next discriminators DD2 – DD5 with true and calculated discriminator outputs.

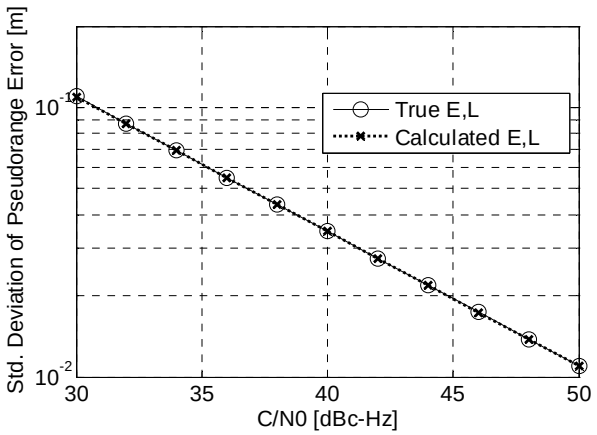

Figure 10. Comparison of the performance of two-channel method, DD1 discriminator and correlator with true *E* and *L* and calculated *E* and *L* outputs; B_n = 3 Hz, T_I = 4 ms.

In Fig. 11. we compare the performance of the receivers equipped with the different discriminators DD1 – DD9. The small differences of the pseudorange errors can be explained by the different sensitivity of the delay discriminators to so called squaring loss and by the different degradation of the discriminator slope caused by the noise.

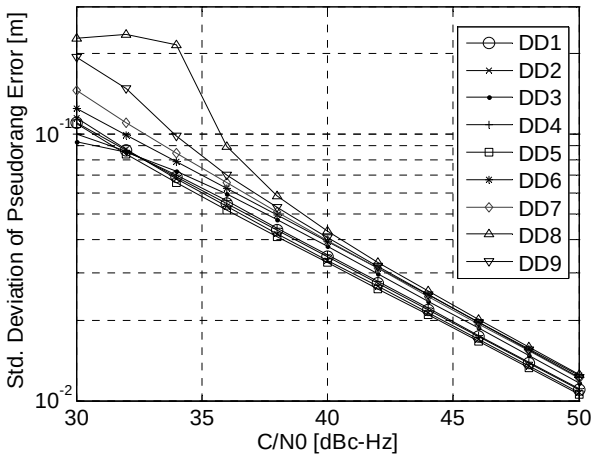

Figure 11. Comparison of the performance of the DD1-DD9; B_n = 3 Hz, T_I = 4 ms.

VIII. CONCLUSION

The paper deals with the processing of the GNSS signal that has power spectrum composed of the two lobes. The overview of the existing methods is given firstly. The existing methods are based on the signal processing theory developed for the first GNSS signals with BPSK modulation. The main result of the paper is the hardware economic two-channel processing method that takes advantage of the spectral property of the signal. The DBBLS signal can be process in two channels without information loss. This approach brings the hardware complexity saving that is reached by the reduction of the processing bandwidth and by the calculation of the early (*E*) and late (*L*) correlatotion products from the prompt (*P*) one.

The developed method can use the existing GNSS chipsets that was developed for processing of the BPSK or QPSK modulated signal for high precision DBBLS signal processing.

The DBBLS signal (BOC, AltBOC,…) processing can be implemented to the simple GNSS receiver hardware, for instance to the Witch Navigator project [9], which is equipped with two relatively narrow band radio channels and medium performance signal processor.

Last, but not least the method can be applied in software GNSS receiver for reduction of the computation complexity.

The other advantage of the developed method is possibility to switch between two processing approaches: a piecewise processing, which is very robust and can operate even if one channel is jammed, and a two-channel cooperative processing, which has a practically the same precision performance as the single-channel receiver. This property can realize the high precise GNSS receivers with high interference immunity that is very important because of the very weak signal level of the GNSS systems.

REFERENCES

[1] G. W. Hein, et al., "Status of Galileo Frequency and Signal Design," *Proceedings of ION 2002* – 24-27 September 2002, Portland, Oregon, USA.

[2] B. C. Barker, et al., "Overview of the GPS M Code Signal," *Proceedings of the 2000 National Technical Meeting of The Institute of Navigation*, Anaheim, CA, January 2000, pp. 542-549.

[3] A. Chen, et al., "GNSS over China, The Compass MEO Satellite codes," *InsideGNSS*, July/August 2007, pp. 36 - 43

[4] N. Shivaramaiah, A. G. Dempster, and C. Rizos, "A hybrid tracking loop architecture for Galileo E5 signal," *in European Navigation Conference,* Naples, Italy, 3-6 May 2009.

[5] A. J. Van Dierendonck, P. Fenton, T. Ford "Theory and Performance of Narrow Correlator Spacing in a GPS Receiver.", *Navigation*, The Institute of Navigation, Alexandria, VA, Vol. 39, No. 3, pp. 265-283.

[6] E. D. Kaplan, Ch Heqarty "Understanding GPS: Principles and Applications, Second Edition.", Artech House 2006, ISBN: 1-58053-894-0.

[7] H. Meyr, H., G. Ascheid, "Synchronization in Digital Communications.Volume I. Phase-, Frequency-Locked Loops and Amplitude Control." John Wiley & Sons, Inc. 1990.

[8] D.M. Akos, A. Ene, J. Thor, "A Prototyping Platform for Multi-Frequency GNSS Receivers," *Proceedings of the 16th International Technical Meeting of the Satellite Division of The Institute of Navigation (ION GPS/GNSS 2003*), Portland, OR, September 2003, pp. 117-128.

[9] O. Jakubov, P. Kovář, P. Kačmařík, F. Vejražka, "The Witch Navigator - a low-cost GNSS software receiver for advanced processing techniques", *Radioengineering. 2010*, vol. 19, no. 4, p. 536-543. ISSN 1210-2512.

[10] P. Kovář, P. P. Kačmařík, F. Vejražka, "High performance Galileo E5 correlator design". *In Proceedings of 13th IAIN World Congress* [CD-ROM]. Bergen: Nordic Institute of Navigation, 2009, p. 1-8.

[11] N. Martin, B Coatantiec, "Method and Device to Compute the Discriminator Function of Signals Modulated with One or More Subcarriers", US Patent 2003/0211580 A1. Dec. 18, 2003.

[12] N. Martin, H. Guichon, M. Revol, "GNSS Receiver with Enhanced Accuracy Using Two Signal Carriers", US Patent 2009/0219201 A1. Sep. 3, 2009.

[13] P. Kovář, P. Kačmařík, F. Vejražka, "Economic Galileo E5 correlator", *Radioengineering.* in press.

[14] Y. Tawk, C. Botteron, A. Jovanovic, P.-A. Farine, "Analysis of Galileo E5 and E5ab Code Tracking.", *GPS Solutions*, Springer, May 2011.